Available online at www.sciencerepository.org

Science Repository

Research Article

A Comprehensive Expression Profile of tRNA-Derived Fragments in Papillary Thyroid Cancer

Shiting Shan, Yuting Wang and Chunfu Zhu*

Department of Pancreas Center, the Affiliated Changzhou No. 2 People's Hospital of Nanjing Medical University, Changzhou, China

ARTICLE INFO

Article history:
Received: 25 July, 2020
Accepted: 24 August, 2020
Published: 28 August, 2020

Keywords:
Papillary thyroid cancer
tRNA-derived fragments
expression profile

ABSTRACT

Objective: In recent years, the incidence of thyroid cancer has been increasing. Papillary thyroid cancer (PTC) is the most common type of malignant thyroid tumor, accounting for approximately 85% of thyroid cancer cases. Although the genetic background of PTC has been studied extensively, relatively little is known about the role of small non-coding RNA (sncRNA) in this disease. tRNA-derived fragments (tRFs) represent a newly discovered class of sncRNAs that exist in many species and play a role in many biological processes.

Methods: In this study, we used RNA sequencing to analyse the expression of tRFs in fresh frozen specimens from PTC tissues and normal tissues adjacent to the tumors. Through this analysis, we identified 49 unique tRFs and transfer RNA halves and then performed quantitative PCR to determine the expression levels of these molecules and to make bioinformatic predictions.

Conclusion: In this report, we provide a comprehensive catalog of tRFs in PTC and assess the abnormal expression of these fragments. These preliminary findings can be used as the basis for further research regarding the functional role of tRFs in patients with PTC.

Introduction

Thyroid cancer, one of the most common malignant tumors in the endocrine system, has demonstrated an annual growth rate of 2% over recent decades [1, 2]. Papillary thyroid cancer (PTC) is the most common type of malignant thyroid tumor, with more than 10 described subtypes of PTC accounting for 85% to 90% of all thyroid malignancies [3, 4]. Fortunately, most PTC tumors are relatively inert, and the 10-year survival rate for patients undergoing glandectomy or total thyroidectomy plus I131 treatment is higher than 95% [5]. In approximately 10% of patients with PTC, however, recurrence or metastasis occurs, necessitating further intervention. Formulating treatments for PTC requires a thorough understanding of the molecular mechanisms behind the pathogenesis and progression of this disease. The genetic background of PTC has been extensively studied; however, relatively little is known about the role of small non-coding RNA (sncRNA) other than microRNA (miRNA) [6].

One avenue of research has led to the discovery of a new class of sncRNA derived from tRNA, known as tRNA-derived fragments (tRFs) [7]. These tRFs have functions similar to those of miRNA, with the ability to directly bind to mRNA, inhibit protein translation, and cleave partially complementary targets [8]. tRFs can regulate gene expression through competitive binding with AGO (Argonaute) family proteins, thereby affecting the silencing efficiency of target genes [9]. In addition, tRFs and its analogs can replace the tumor gene mRNA binding protein YBX1, blocking its interaction with oncogenic mRNA and destabilizing oncogene mRNAs, resulting in inhibition of tumor cell infiltration [10]. tRFs can also regulate protein biosynthesis by affecting the translation mechanism and can regulate ribosome biogenesis at different levels. Research has also shown that tRF can be used as a guide RNA in viral

**Correspondence to:* *Chunfu Zhu, Department of Pancreas Center, the Affiliated Changzhou No. 2 People's Hospital of Nanjing Medical University, Changzhou, 213003, China; E-mail: zcfmlm@njmu.edu.cn*

http://dx.doi.org/10.31487/j.JSO.2020.04.08

reverse transcription (RT) and can be combined with primer RNA to initiate RT. When combined with cytochrome C, tRFs inhibit the formation of apoptotic bodies. Finally, studies have shown that tRF exists in hematopoietic cells, lymphocytes, and the blood circulation system, suggesting that these fragments may play a role in immune response [11-13].

Previous research has shown that the underlying mechanism of tRF regulates various human diseases such as cancers, pathological stress injuries, metabolic diseases, viral infections, and nervous system diseases [14-16]. However, the understanding of how tRF regulates cancer progression is still in its infancy [17]. Previous studies have shown that tRFs and transfer RNA halves (tiRNAs) are seen in breast cancer, prostate cancer, colorectal cancer, liver cancer, and pancreatic cancer, but the potential role of tRFs and tiRNAs in thyroid cancer has not yet been reported [18-20]. In this study, we therefore, sought to explore the expression and function of how to regulate cancers in patients with PTC.

Materials and Methods

I Sample Collection

Four patients (1 woman, 3 men; age range, 30-50 years), all of whom had undergone surgery for PTC at the Affiliated Changzhou No. 2 People's Hospital of Nanjing Medical University (Jiangsu, China), were recruited in 2019 for participation in this study. They have no underlying disease and no history of other operations. After the operation, they received endocrine replacement therapy. Each patient provided written informed consent, and the ethics committee of Changzhou Second People's Hospital affiliated to Nanjing Medical University approved the study protocol. The stage of PTC for each patient was determined based on the thyroid cancer TNM staging system published by the American Joint Committee on Cancer in 2017 (Table 1) [21]. Four pairs of PTC specimens and adjacent tissues (distance of 2 cm from the tumor; used a control group) were collected after surgery for tRF and tiRNA sequencing; these samples were immediately stored in liquid nitrogen at 80°C.

Table 1: Patient and tumor characteristics.

Patient number	Age (years)	Sex	Tumor size (cm)	Tumor stage	Pathological description of tumor
1	45	Male	0.6	T1N0M0	Mini papillary carcinoma, no lymph node metastasis
2	37	Male	1.2	T1N1M0	Papillary carcinoma, left central lymph node 1/1 metastasis
3	48	Male	2.5	T2N0M0	Papillary carcinoma, no lymph node metastasis, tumor invasion of left recurrent laryngeal nerve
4	67	Female	0.9	T1N1M0	Papillary carcinoma, 1/4 lymph node metastasis in the central area, 1/1 lymph node metastasis in the left 2A area, and 6/19 lymph node metastasis in the left 4 area

T: tumor; N: node; M: metastasis.

II tRNA-Derived Small RNA (tsRNA) Types

The types of tsRNA are divided into 5 categories based on the cleavage site of the precursor or mature RNA transcript:

i. 5'-half: A 5'-tRNA half-molecule tiRNA that is produced by angiogenin (ANG) specifically cleaving at the anticodon loop of mature tRNA under various stress conditions.
ii. 3'-half: A 3'-tRNA half-molecule tiRNA that is produced by ANG specifically cleaning at the anticodon loop of mature tRNA under various stress conditions.
iii. 5'-tRF: A fragment from mature tRNA in which the 5' end is cleaved at the D-loop or anticodon stem.
iv. i-tRF: A fragment originating from the inside of mature tRNA; and
v. 3'-tRF: The 3' end of mature tRNA occurring at the T-loop or anticodon molecules cut at the stem (Figure 1).

The same type of tsRNA can be cut from multiple tRNAs, but the functions of tsRNA from different tRNA sources vary.Different types of tRF have different biological functions. tiRNA can reduce the overall translation speed by 10% to 15%; part of the 5'-tiRNA from tRNAAla and tRNACys can be assembled into a G4 motif to competitively bind eIF4G/eIF4A in the translation initiation complex, thereby inhibiting Cap-dependent mRNA translation. The known tRNA ratio distribution is shown in (Figure 2), and the known tsRNA ratio distribution is shown in (Figure 3). As a sncRNA, the length of mature tsRNA generated by tRNA shearing generally ranges from 16 to 35 nts (Figure 4).

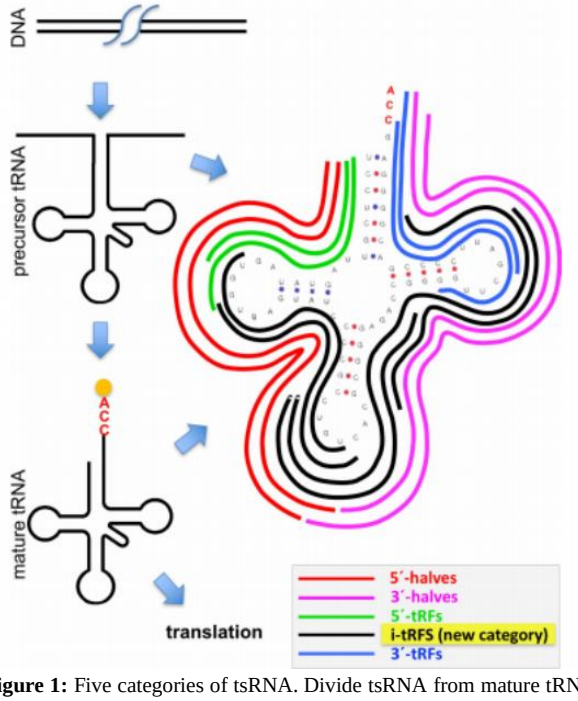

Figure 1: Five categories of tsRNA. Divide tsRNA from mature tRNA into five categories: 1) 5'-half: as shown in the red part of Figure 1; 2) 3'-half: as shown in the magenta part of Figure 1; 3) 5'-tRF: as shown in the green part of Figure 1; 4) i-tRF: as shown in the black part of Figure 1; 5) 3'-tRF: as shown in the blue part of Figure 1.

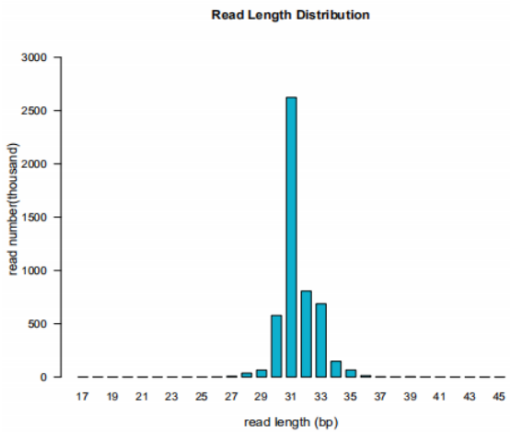

Figure 2: Statistics of known tsRNA length. The length distribution of mature tsRNA generated by tRNA shearing is shown in Figure 2. The length of tsRNA is mainly concentrated in the range of 16 to 35 nts.

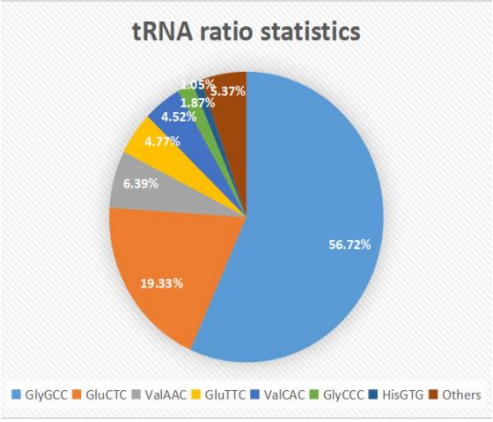

Figure 3: Statistics of the number of known tRNA. The known tRNA ratio distribution is shown in Figure 3: the light blue part represents the proportion of GlyGCC, the orange part represents GluCTC, the gray part represents ValAAC, the yellow part represents GluTTC, the blue part represents VAlCAC, the green part represents GlyCCC, dark blue The colour part represents HisGTG, and the brown part represents other.

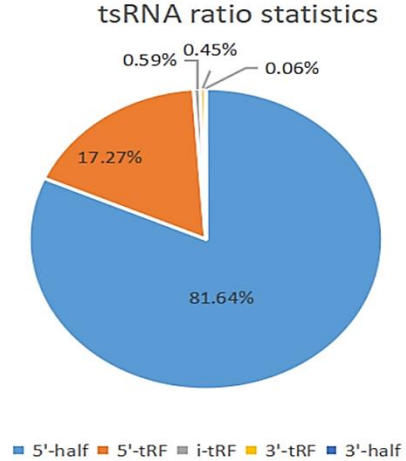

Figure 4: Statistics of the number of known tsRNA. The known tsRNA ratio distribution is shown in Figure 4: the light blue part represents the proportion of 5'-half, the orange part represents 5'-tRF, the gray part represents i'-tRF, and the yellow part represents 3'-tRF, The blue part represents 3'-half.

III tRF and tiRNA Sequencing

Because tRFs are short fragments, the library was constructed as follows: the total RNA of the sample or the purified sRNA fragment was extracted, with the 3' end and the 5' connector joined successively. RT into cDNA was performed, followed by PCR expansion. The target fragment library was then recovered via gel cutting, and the library was sequenced on the computer. Illumina HiSeq 2500 was used to sequence the raw data (raw reads). The joints at both ends of the reads were removed; low-quality reads and reads with a fragment length < 15 nt were also removed to complete the initial data filtering and obtain high-quality data (clean reads). Clean reads were then compared with the reference genome to obtain a genome-wide read distribution map, and clean reads were annotated according to ncRNA classification. The expressions of identified tsRNA and cluster tsRNA were calculated, and tsRNA was analysed for differential expression between samples.

IV RT: Quantitative PCR (q-PCR)

We selected 4 tRFs and tiRNAs for PCR verification. First, we extracted total RNA from PTC cells and normal thyroid cells using RL lysate. The RNA was reverse transcribed (at 42°C for 60 min followed by 70°C for 10 min) using the Bulge-Loop miRNA q RT-PCR Starter Kit (Guangzhou Ruibo Bio Co., Ltd). Then, the qPCR was performed with U6 small nuclear RNA (snRNA) as an internal control. After adding the forward primer, reverse primers (designed specifically for each tRF by Ribobio), and cDNA, the PCRs were incubated at 95°C for 10 min, followed by 60 cycles of 95°C for 2 s, 60°C for 20 s, and 70°C for 10 s in the Roche LightCycler 480 Real-Time PCR System (Roche LightCycler® 480 system, Basel, Switzerland). Finally, the results were calculated by the $-\Delta\Delta$ 2 Ct method to analyse the expression of each specific tDR in different samples.

V Predicted Targets of tRFs and tiRNAs

sRNA target gene prediction mainly considers the complementary pairing of tsRNA and mRNA 3′ untranslated regions. Different software programs predict different target genes based on the complementary pairing of tsRNA and its target site. We used 3 software programs to predict targets: MiRanda (Link 1), RNAhybrid (Link 2), and targetScan (Link 3). We then screened and sorted the results from the 3 programs, using the prediction results as the candidate target genes of tsRNA.

VI Functional tRF and ti-RNA Enrichment Analysis

Biological pathway analysis was based on the Kyoto encyclopedia of genes and genomes (KEGG) Biological Pathway Database (Link 4). We placed the candidate target genes into the biological pathway for comprehensive analysis and analysed the degree of influence and regularity of the functional variation on the biological pathway. The gene function enrichment analysis process was thus divided into 2 steps: a KEGG biological pathway annotation and an enrichment analysis. For this analysis, the P value was calculated using Fisher's exact test, with $P < 0.05$ used as the significance threshold. Significant signal transduction and disease pathways were identified, thereby providing distribution information and significance status for gene sets in the KEGG category. Gene ontology (GO) analysis was used to perform functional annotation

on each gene and to calculate the most significant function in a specific series of genes through statistical analysis (e.g., using hypergeometric distribution). The lower the P value, the greater the significance of the GO term ($P \leq 0.05$ was suggested as the threshold for significance).

Results

I tRF and tiRNA Sequencing

The expression of various samples is shown in (Figure 5). Using a P value < 0.05, we selected a total of 49 DE-tRFs and tiRNAs, including 27 down-regulated tRFs and tiRNAs and 22 up-regulated tRFs and tiRNAs (Table 2).

Table 2: tRFs and tiRNAs selected for validation via quantitative PCR.

tsRNA_ID	tRNA	tsRNA_type	Sequence
tRF-27-PIR8YP9LON3	GlyCCC	5'-tRF	GCACTGGTGGTTCAGTGGTAGAATTCT
tRF-34-YSV4V47Q2WW1J1	ValCAC	i-tRF	TTCCGTAGTGTAGTGGTTATCACGTTCGCCTCAC
tRF-38-0VL8K87SIRMM12V	GluCTC	3'-tRF	ACCGCCGCGGCCCGGGTTCGATTCCCGGTCAGGGAACC
tRF-39-0VL8K87SIRMM12E2	GluCTC	3'-tRF	ACCGCCGCGGCCCGGGTTCGATTCCCGGTCAGGGAACCA

tRF: transfer RNA-derived fragment; tiRNA: transfer RNA half; tsRNA: tRNA-derived small RNA; i-tRF: tRNA half.

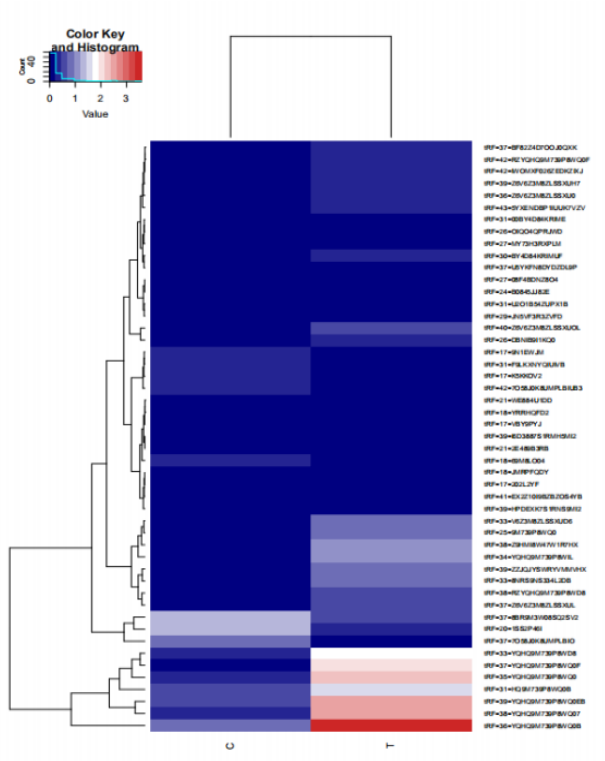

Figure 5: tsRNA heat map of different expression levels between samples. Heat map indicating the expression levels of various tRFs and tiRNAs. Brick red represents high expression of tsRNA in the sample; navy blue represents low expression. Each square represents a gene, and its colour represents the amount of expression of the gene. The higher the amount of expression, the darker the colour.

II RT-qPCR

For further qPCR verification, we chose 4 DE-tRFs and tiRNAs (tRF-38-0VL8K87SIRMM12V, tRF-39-0VL8K87SIRMM12E2, tRF-27-PIR8YP9LON3, and tRF-34-YSV4V47Q2WW1J1). These sequences were significantly different between the thyroid cancer specimens and the adjacent normal tissue specimens and presented abundant expression. qPCR demonstrated that tRF-38-0VL8K87SIRMM12V and tRF-34-YSV4V47Q2WW1J1 were up-regulated and tRF-39-0VL8K87SIRMM12E2 and tRF-27-PIR8YP9LON3 were down-regulated in the thyroid cancer tissue samples compared with the adjacent normal tissue samples (Table 3), findings consistent with the sequencing results shown in (Table 4). However, because of the small sample size, the P values did not indicate statistical significance for these differences.

III Predicted Targets of Functional DE-tRF and ti-RNA Enrichment Analysis

Figure 6 shows the intersection of the target genes of tsRNA from the 3 software programs used in the study. For target gene prediction, tRF-39-0VL8K87SIRMM12E2 was predicted to have 553 target genes by miRanda, RNAhybrid, and TargetScan. KEGG analysis was then performed on the target genes; an example of KEGG channel analysis results is shown in (Figure 7). tRF-39-0VL8K87SIRMM12E2 was mostly enriched in the "Metabolic Pathways" section of the figure. In (Figure 8), a candidate target gene KEGG pathway bubble chart shows the proportion of enriched differential genes in the background genes of the pathway.

Table 3: Quantitative PCR results for tRFs and tiRNAs selected for validation.

tsRNA_ID	tRNA	tsRNA type	Fold change, T/N	*P* value
tRF-27-PIR8YP9LON3	GlyCCC	5'-tRF	0.7583	0.010854034
tRF-34-YSV4V47Q2WW1J1	ValCAC	i-tRF	1.9830	0.032495249
tRF-38-0VL8K87SIRMM12V	GluCTC	3'-tRF	2.6790	0.039325243
tRF-39-0VL8K87SIRMM12E2	GluCTC	3'-tRF	0.2602	0.040483666

tRF: transfer RNA-derived fragment; tiRNA: transfer RNA half; tsRNA: tRNA-derived small RNA; T/N: tumor/normal tissue; i-tRF: tRNA half.

Table 4: The 49 tRFs and tiRNAs expressed within thyroid cancer samples.

tsRNA_ID	tRNA	tsRNA type	Fold change, T/N	*P* value
Up-regulated tsRNA				
tRF-36-EX2Z10I9BZBZOSD	GluCTC	3'-tRF	2.7850	0.040483666
tRF-34-YSV4V47Q2WW1J1	ValCAC	i-tRF	2.7650	0.032495249
tRF-21-Q622EVUID	SerGCT	i-tRF	2.7127	0.007831404
tRF-19-6998LOJX	ArgTCT	5'-tRF	2.5443	0.009509807
tRF-42-JMRPFQJDZXHY13KKN	LysTTT	i-tRF	1.6630	0.039598115
tRF-32-WP9N1EWJQ72SJ	GluCTC	i-tRF	1.6540	0.014928189
tRF-18-9EDJSYDE	ArgCCG	i-tRF	1.5430	0.025013166
tRF-24-3RUJJKIWIZ	ArgCCT	i-tRF	0.5850	0.01396513
tRF-20-K0JNORRN	GlyTCC	i-tRF	0.5850	0.0146963
tRF-29-247383RPD9JM	GluTTC	i-tRF	0.5850	0.01650732
tRF-21-DBNIB9I1D	SerGCT	i-tRF	0.5850	0.01976722
tRF-26-Z9HMI8W47WB	GluTTC	i-tRF	0.5850	0.021853102
tRF-24-XW7616MSIZ	TrpCCA	i-tRF	0.5850	0.041615961
tRF-34-VF4YO9XEKJ5RHZ	GlnCTG	i-tRF	0.5850	0.042128818
tRF-40-2VR008R9D9KUMKF6	AspGTC	3'-half	0.4514	0.047686582
tRF-27-PW5SVP9N155	HisGTG	5'-tRF	0.3583	0.047326167
tRF-29-6XQ6S8V0J8HW	LysCTT	i-tRF	0.1500	0.03027957
tRF-18-D5YEYYD2	TrpTCA	3'-tRF	0.1155	0.032765666
tRF-31-ZRS3SJRX8FYVD	ValCAC	i-tRF	0.0589	0.033733536
tRF-33-KY7343RX6NMHD5	GluCTC	i-tRF	0.0489	0.037522167
tRF-43-96L85DMKYUYRLHR0D2	AspGTC	3'-half	0.0395	0.032938657
tRF-33-V29K9UV36562DE	GlnTTG	5'-half	0.0091	0.037196629
Down-regulated tsRNA				
tRF-39-0VL8K87SIRMM12E2	ValTAC	i-tRF	–0.0780	0.022305473
tRF-33-2QR7F8YKIR9N05	GluTTC	i-tRF	–0.0973	0.020345176
tRF-28-389MV47P59D9	GluCTC	i-tRF	–0.1227	0.044529882
tRF-19-27NXJ4E2	LysTTT	3'-tRF	–0.4150	0.006379632
tRF-24-04SXQ3V2KJ	GluTTC	i-tRF	–0.4739	0.018091021
tRF-33-QKF1R3WE8RO8DX	AspGTC	i-tRF	–0.5391	0.034026498
tRF-23-9MV4QP59D9	GluTTC	i-tRF	–0.5850	0.012035638
tRF-35-L85J3KYUYR66IF	GlyGCC	i-tRF	–0.5850	0.029210898
tRF-27-78WPRLXN48Q	ProTGG	i-tRF	–0.5850	0.032259404
tRF-23-UJJKIWRNDL	ArgCCT	i-tRF	–0.5850	0.039406883
tRF-18-8L8NRS04	GluTTC	i-tRF	–0.5850	0.040329745
tRF-28-V2Y8L981PVD9	GluCTC	i-tRF	–0.5850	0.042980739
tRF-28-8URUZ9HNONDU	CysGCA	i-tRF	–0.5850	0.043138681
tRF-26-2IU5YKFN8DE	ValTAC	i-tRF	–0.6630	0.046193757
tRF-26-1IUUK7VZ0RB	HisGTG	3'-tRF	–0.7370	0.011287299
tRF-19-OB9ZFHIW	PheGAA	i-tRF	–0.8480	0.037241975
tRF-24-7OHFO6FJH5	TrpTCA	i-tRF	–1.5370	0.045634736
tRF-28-V6Z3M8ZLSS0M	GluTTC	i-tRF	–1.5496	0.018644108
tRF-25-INVDRI2Q2R	PheGAA	i-tRF	–1.5850	0.022304427
tRF-24-86J8WPMNEX	GluTTC	5'-tRF	–1.5850	0.033672616
tRF-28-DBNIB9I1KQ0D	SerGCT	i-tRF	–1.6323	0.015290674
tRF-37-2S3HPSR95933JKF	GluCTC	i-tRF	–2.1560	0.039608438
tRF-17-3SNKP92	ThrTGT	3'-tRF	–2.3850	0.044427453
tRF-39-PNR8YP9LON4VN1EM	GlyGCC	5'-tRF	–2.8413	0.004510105
tRF-27-PIR8YP9LON3	GlyCCC	5'-tRF	–2.9430	0.010854034
tRF-38-0VL8K87SIRMM12V	GluCTC	3'-tRF	–2.9860	0.039325243
tRF-22-MI7O3B1N4	AsnGTT	i-tRF	–3.2150	0.041341606

tRF: transfer RNA-derived fragment; tiRNA: transfer RNA half; tsRNA: tRNA-derived small RNA; T/N: tumor/normal tissue; i-tRF: tRNA half.

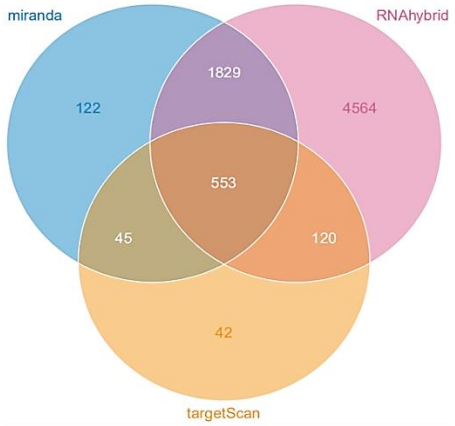

Figure 6: Target Gene Prediction Venn Diagram. The intersection of the target genes of tsRNA shown in the Venn diagram (Venn/Venn diagram) in the three softwares.

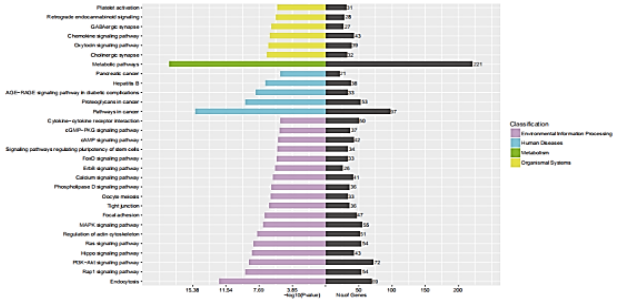

Figure 7: Enrichment diagram of KEGG pathway between samples. In the figure, the purple part represents Environmental information processing, the blue part represents Human disease, the green part represents metabolism, and the yellow part represents Organicismal Systems.

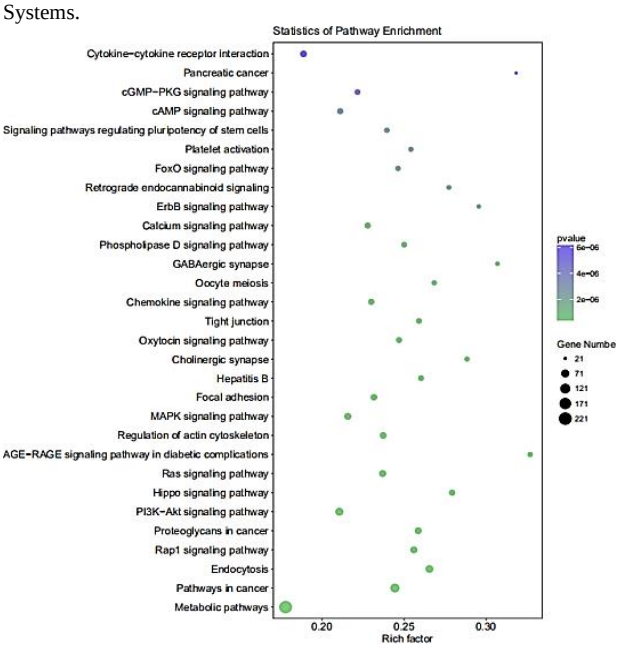

Figure 8: Candidate target gene KEGG pathway bubble chart. In the figure, the abscissa indicates the ratio of enriched differential genes to the background genes of the pathway, and the ordinate indicates the pathway name; the size of the dots in the graph indicates the number of enriched differential genes, and the colour indicates the P value.

Discussion

As sequencing technology has improved, research into sncRNA has progressed, bringing about the discovery of tRFs [22]. Since the initial discovery of these fragments, tRFs have been described in many species and organisms, including in various cancer cell lines [23]. More specifically, research has shown that some tRFs may play a role in cancer suppression by combining with the mRNA binding protein YBX1, which is highly overexpressed in many cancer types and has been implicated in many key cellular pathways [24]. In colorectal cancer, the combination of tRF and miR-1280 has been found to suppress cancer growth and metastasis by repressing Notch signaling pathways that support CSC phenotypes [25]. Other research has demonstrated that tRF is out of expression in patients with prostate cancer, with survival curve analysis showing that tRF expression affects both progression-free survival and prognosis [26].

In this study, we explored the composition and expression of tRFs in patients with PTC. We screened 49 DE-tRFs and tiRNAs from thyroid cancer samples and adjacent normal tissues, including 27 down-regulated tRFs and tiRNAs and 22 up-regulated tRFs. Through qPCR verification, we confirmed that tRF-34-YSV4V47Q2WW1J1 and tRF-38-0VL8K87SIRMM12V are up-regulated in PTC, whereas tRF-39-0VL8K87SIRMM12E2 and tRF-27-PIR8YP9LON3 are down-regulated, findings consistent with our sequencing data. After repeated qPCR verification, the largest expression difference between thyroid cancer samples and adjacent normal tissue samples was seen with tRF-39-0VL8K87SIRMM12E2. In addition, we used the software programs MiRanda, RNAhybrid, and targetScan to predict the targets of differentially expressed tiRNAs and tRFs. This analysis confirmed that the down-regulated tRF-39-0VL8K87SIRMM12E2 was mainly involved in metabolic pathways and in cancer-related signaling pathways. Previous research has addressed the effect of tRF on tumor occurrence and development, but little is known regarding how tRFs affect the metabolic pathways.

Based on the results of this study, we suggest that further research is needed regarding how tRFs affect the occurrence and development of PTC by affecting biological metabolism. In the near future, we plan to conduct such research to confirm and expand on these findings. This study had several limitations. The results are based only on tRF and tiRNA sequencing analysis and bioinformatics prediction and require validation. The small sample size of the study led to large statistical differences between samples; further studies in large clinical cohorts will be required.

Conclusion

In this study, we provided a comprehensive expression profile of tRFs in PTC and identified several potential avenues of further research.

Data Availability

For more information on how to compose a data availability statement, including template examples, please visit: Link 5.

Conflicts of Interest

None.

Acknowledgments

This study was supported by the Social Development Foundation of Science and Technology of Jiangsu (BE2016658), the Changzhou Sci & Tech Program (CE20165020), the High-Level Medical Talents Training Project of Changzhou (2016CZLJ007), and the Project of Changzhou medical innovation team (CCX201807).

References

1. Hyeyeun Lim, Susan S Devesa, Julie A Sosa, David Check, Cari M Kitahara (2017) Trends in Thyroid Cancer Incidence and Mortality in the United States, 1974-2013. *JAMA* 317: 1338-1348. [Crossref]
2. Sabri Özden, Bülent Çomçalı, Hakan Ataş, Sadettin Er, Mesut Tez et al. (2020) A Diagnostic Dilemma: Skip Metastasis in Papillary Thyroid Cancer. *Am Surg* 86: 245-249. [Crossref]
3. Ziyang Huang, Muye Song, Shujie Wang, Jianhao Huang, Hongyan Shi et al. (2020) Preoperative serum thyroglobulin is a risk factor of skip metastasis in papillary thyroid carcinoma. *Ann Transl Med* 8: 389. [Crossref]
4. Agnieszka Zembska, Aleksandra Jawiarczyk Przybyłowska, Beata Wojtczak, Marek Bolanowski (2019) MicroRNA Expression in the Progression and Aggressiveness of Papillary Thyroid Carcinoma. *Anticancer Res* 39: 33-40. [Crossref]
5. Toshihiko Sakai, Iwao Sugitani, Aya Ebina, Osamu Fukuoka, Kazuhisa Toda et al. (2019) Active Surveillance for T1bN0M0 Papillary Thyroid Carcinoma. *Thyroid* 29: 59-63. [Crossref]
6. Francesca Rosignolo, Lorenzo Memeo, Fabio Monzani, Cristina Colarossi, Valeria Pecce et al. (2017) MicroRNA-based molecular classification of papillary thyroid carcinoma. *Int J Oncol* 50: 1767-1777. [Crossref]
7. Zhongliang Ma, Jinbao Zhou, Yang Shao, Fatemah A Jafari, Pengfei Qi et al. (2020) Biochemical properties and progress in cancers of tRNA-derived fragments. *J Cell Biochem* 121: 2058-2063. [Crossref]
8. Zhangli Su, Elizabeth L Frost, Catherine R Lammert, Roza K Przanowska, John R Lukens et al. (2020) tRNA-derived fragments and microRNAs in the maternal-fetal interface of a mouse maternal-immune-activation autism model. *RNA Biol* 17: 1183-1195. [Crossref]
9. Marek Kazimierczyk, Agata Jędroszkowiak, Dorota Kowalczykiewicz, Maciej Szymański, Barbara Imiołczyk et al. (2019) tRNA-derived fragments from the Sus scrofa tissues provide evidence of their conserved role in mammalian development. *Biochem Biophys Res Commun* 520: 514-519. [Crossref]
10. Huimin Shi, Minyi Yu, Yue Wu, Yuepeng Cao, Shanwen Li et al. (2020) tRNA-derived fragments (tRFs) contribute to podocyte differentiation. *Biochem Biophys Res Commun* 521: 1-8. [Crossref]
11. Fudi Zhong, Zhigao Hu, Keqing Jiang, Biao Lei, Zhan Wu et al. (2019) Complement C3 activation regulates the production of tRNA-derived fragments Gly-tRFs and promotes alcohol-induced liver injury and steatosis. *Cell Res* 29: 548-561. [Crossref]
12. Juan Pablo Tosar, Alfonso Cayota (2020) Extracellular tRNAs and tRNA-derived fragments. *RNA Biol* 17: 1149-1167. [Crossref]
13. J A Green, M Y Ansari, H C Ball, T M Haqqi (2020) tRNA-derived fragments (tRFs) regulate post-transcriptional gene expression via AGO-dependent mechanism in IL-1beta stimulated chondrocytes. *Osteoarthritis Cartilage* 28: 1102-1110. [Crossref]
14. Yue Huang, Han Ge, Mingjie Zheng, Yangyang Cui, Ziyi Fu et al. (2020) Serum tRNA-derived fragments (tRFs) as potential candidates for diagnosis of nontriple negative breast cancer. *J Cell Physiol* 235: 2809-2824. [Crossref]
15. Mehmet Ilyas Cosacak, Ipek Erdogan, Ayten Nalbant, Bunyamin Akgul (2018) Small RNA data set that includes tRNA-derived fragments from Jurkat cells treated with camptothecin. *Data Brief* 17*:* 397-400. [Crossref]
16. Tianyu Zeng, Yijia Hua, Chunxiao Sun, Yuchen Zhang, Fan Yang et al. (2020) Relationship between tRNA-derived fragments and human cancers. *Int J Cancer*. [Crossref]
17. Eric Londin, Rogan Magee, Carol L Shields, Sara E Lally, Takami Sato et al. (2020) IsomiRs and tRNA-derived fragments are associated with metastasis and patient survival in uveal melanoma. *Pigment Cell Melanoma Res* 33: 52-62. [Crossref]
18. E S Martens Uzunova, S E Jalava, N F Dits, G J L H van Leenders, S Møller et al. (2012) Diagnostic and prognostic signatures from the small non-coding RNA transcriptome in prostate cancer. *Oncogene* 31: 978-991. [Crossref]
19. Hani Goodarzi, Xuhang Liu, Hoang C B Nguyen, Steven Zhang, Lisa Fish et al. (2015) Endogenous tRNA-Derived Fragments Suppress Breast Cancer Progression via YBX1 Displacement. *Cell* 161: 790-802. [Crossref]
20. Lei Jin, Chunfu Zhu, Xihu Qin (2019) Expression profile of tRNA-derived fragments in pancreatic cancer. *Oncol Lett* 18: 3104-3114. [Crossref]
21. Mohamed Abdelgadir Adam, Samantha Thomas, Sanziana A Roman, Terry Hyslop, Julie A Sosa (2017) Rethinking the Current American Joint Committee on Cancer TNM Staging System for Medullary Thyroid Cancer. *JAMA Surg* 152: 869-876. [Crossref]
22. Yangyang Cui, Yue Huang, Xiaowei Wu, Mingjie Zheng, Yiqin Xia et al. (2019) Hypoxia-induced tRNA-derived fragments, novel regulatory factor for doxorubicin resistance in triple-negative breast cancer. *J Cell Physiol* 234: 8740-8751. [Crossref]
23. Bingqing Huang, Huipeng Yang, Xixi Cheng, Dan Wang, Shuyu Fu et al. (2017) tRF/miR-1280 Suppresses Stem Cell-like Cells and Metastasis in Colorectal Cancer. *Cancer Res* 77: 3194-3206. [Crossref]
24. Michael Olvedy, Mauro Scaravilli, Youri Hoogstrate, Tapio Visakorpi, Guido Jenster et al. (2016) A comprehensive repertoire of tRNA-derived fragments in prostate cancer. *Oncotarget* 7: 24766-24777. [Crossref]
25. Nicola Guzzi, Cristian Bellodi (2020) Novel insights into the emerging roles of tRNA-derived fragments in mammalian development. *RNA Biol* 17: 1214-1222. [Crossref]
26. Simon P Keam, Gyorgy Hutvagner (2015) tRNA-Derived Fragments (tRFs): Emerging New Roles for an Ancient RNA in the Regulation of Gene Expression. *Life* 5: 1638-1651. [Crossref]